26th EPS Conf. on Contr. Fusion and Plasma Physics, Maastricht, 14 - 18 June 1999 ECA Vol.23J (1999) 1509 - 1512

Deuterium inventories in different divertor configurations of ASDEX Upgrade

H. Maier, K. Krieger, A. Tabasso, S. Lindig, V. Rohde, J. Roth,
and the ASDEX Upgrade Team

Max-Planck-Institut für Plasmaphysik, EURATOM Association, Garching, Germany

The formation of co–deposited carbon hydrate layers in the divertor area of fusion experiments addresses a serious problem for future fusion devices. A detailed understanding of the mechanisms leading to their formation is necessary because such layers will contain permanent tritium inventories in future devices [1]. In this contribution deuterium inventories for two different divertor configurations of ASDEX Upgrade are discussed and compared.

ASDEX Upgrade was originally equipped with flat target plates made of fine grain graphite. During the 1995/1996 experimental campaign the graphite strike point areas were replaced by toroidal belts of tiles covered with a plasma sprayed tungsten layer.

Since the summer of 1997 the tokamak is operated with a new nearly vertically arranged divertor configuration. An overview of the two geometries is shown in figure 1 together with the respective coordinates along the target plate surfaces. Also shown is the tilted mounting geometry of the tungsten tiles in Divertor I.

We compare the deuterium inventories in these different divertor configurations. The near surface deuterium content of the tiles is analyzed utilizing the nuclear reaction method ^{3}He(d,p)α. The cross section of this reaction is such that for an incident ^{3}He ion energy of about 800 keV a surface layer with a thickness in the range of 1 μm can be investigated, depending on the composition of the deposited layers. The results on the Divertor I configuration presented here have all been determined from samples

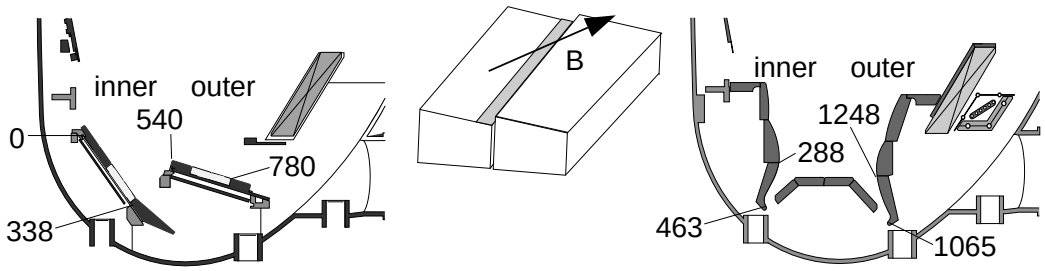

Figure 1: *Poloidal sections of Divertor I (left) and Divertor II (right) of ASDEX Upgrade. The numbers denote the coordinate "s" in mm , which represents the distance along the target plates. The lighter regions in the left plot denote the tungsten covered surfaces. In the middle the tilted toroidal mounting of the tungsten tiles is displayed.*

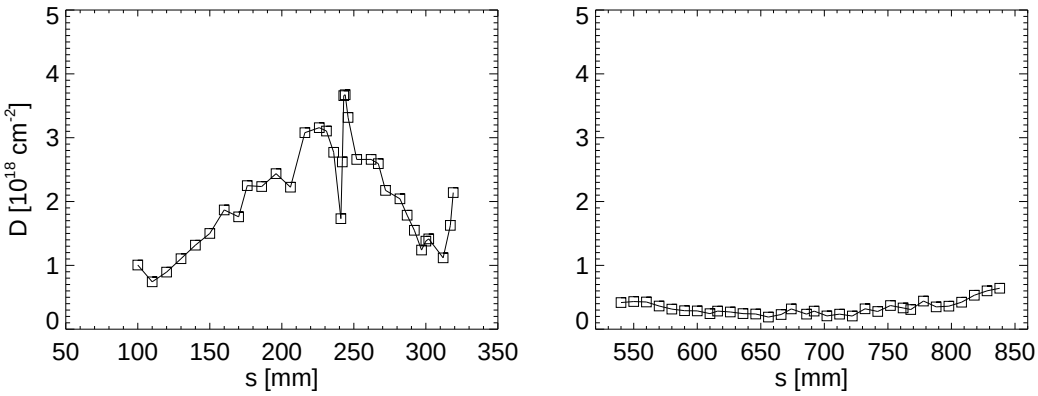

Figure 2: *Near surface deuterium inventory on ASDEX Upgrade graphite target plates in the Divertor I configuration after the tungsten divertor experiment. Left: Inner target plate. Right: Outer target plate.*

taken after the tungsten experimental campaign. Analysis of graphite target plates was possible because a special set of tiles employed for infrared thermography had not been replaced by tungsten covered tiles. Therefore we can compare the deuterium retention on graphite and on tungsten samples, which all had undergone the same "history" of discharges.

Figure 2 displays the near surface D inventory found on graphite for the inner and outer divertor target plate, respectively. A pronounced maximum can be observed in the region of high plasma fluence for the inner target plate. The opposite can be observed on the righthand side for the outer divertor: A broad and shallow minimum. If we assume co–deposition of D with carbon to be the dominant mechanism for building up large D inventories, these results indicate that deposition prevails in the inner divertor, while hardly any deposition occurs on the outboard side.

This conclusion can be further investigated in the case of the tungsten covered tiles. As in the above case, figure 3 displays a significantly larger D inventory in the inner divertor as compared to the outer. In addition, however, there is a pronounced shadowing effect which results from the inclined mounting of adjacent tiles. The insets display the total amounts of low-Z material deposited onto the tungsten surfaces in the shadowed and plasma–exposed regions on the respective tiles. These data were obtained by integrating depth profiles from 2 MeV proton RBS [2]. By comparing the insets with the main figures, a correlation between deuterium retention and the presence of deposited low-Z layers can be observed. Note however, that the thicker layers on the plasma–exposed side of the inner tile contain less D than the shadowed portions. This indicates a lower D/C ratio which is presumably due to higher surface temperatures.

Figure 4 shows the D inventories measured in the Divertor II configuration after the first experimental campaign 1997/1998. The average strike positions of the plasma

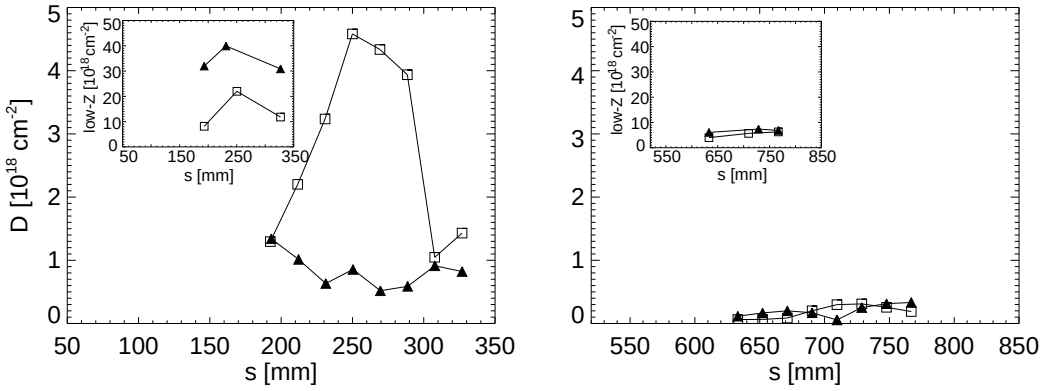

Figure 3: *Near surface deuterium inventory on ASDEX Upgrade tungsten target plates in the Divertor I configuration after the tungsten divertor experiment. Left: Inner target plate. Right: Outer target plate. The figures display the inventories of the plasma exposed (solid triangles) and shadowed (open sqares) regions (see fig. 1) separately for the respective tiles. The insets show the corresponding total amount of deposited low–Z material (same symbols and units). See text.*

fan are located in the vicinity of s=400 mm for the inner and s=1100 mm for the outer module, respectively. As the figure shows, local maxima can be observed at these locations in both cases. According to the findings discussed above, this can be interpreted as deposition of carbon occuring in the outer as well as in the inner divertor. The maxima around s=460 mm and s=1060 mm are clearly not correlated with the strike positions of the plasma fan, but are located at the lower rounded edges of the modules. This indicates that such layers are not directly created by co–deposition with carbon impurities from the plasma, since the direct plasma fluence onto these positions is very low.

An attempt to model this difference of erosion/deposition patterns in the two diver-

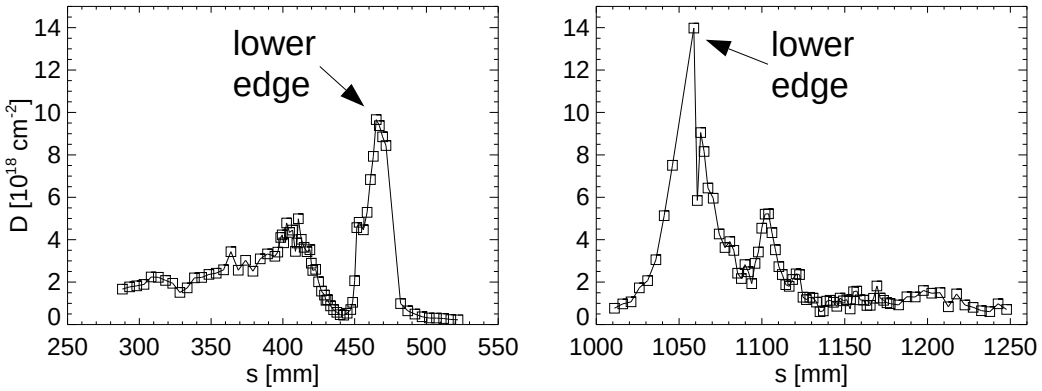

Figure 4: *Near surface deuterium inventory on ASDEX Upgrade CFC graphite target modules in the Divertor II configuration. Left: Inner target plate. Right: Outer target plate.*

tor configurations in detail would be difficult, since the respective target plates had been subjected to a variety of different discharge conditions. Therefore we compare these results with an analytical model [3], which is based on numerical simulations and employs only the local values of impurity concentration and electron temperature of a plasma impinging on a surface to predict erosion/deposition. Plasma carbon concentrations of about 0.5 %-1.5 % are found in the main plasma for Divertor I [4]. For the carbon strike point modules of Divertor II we assume these values to represent a lower limit of C concentrations. To derive an estimate of the respective electron temperatures representative for the case of our study, we performed a flux–weighted average of target plate Langmuir probe data from about 300 discharges for each divertor configuration. The resulting values are 8 eV/16 eV for the inner/outer divertor in configuration I and 10 eV/9 eV in configuration II. With these data sets the model predicts deposition on the inner target for the Divertor I configuration and on both targets for Divertor II. Only in the outer divertor of the Divertor I configuration the average plasma temperature exceeds the limit for deposition and the model predicts erosion. These predictions are in agreement with the results described above. The model does, however, not include the contribution of chemical erosion of carbon.

Finally, the composition of layers formed at non–plasma–exposed surfaces was investigated. After the 1997/1998 campaign a metal strip was removed from the bottom of the vessel below the divertor. Samples taken from this strip were analyzed for their elemental composition. Apart from hydrogen isotopes, the layers consisted of 50-55 % C containing O and B to amounts of 10 % and 5 %, respectively. To measure H and D separately, the method of elastic recoil detection analysis (ERDA) was employed. The observed amounts of 15-20 % for H and 17-27 % for D result in an average ratio of (H+D)/C of up to 0.8. From this number it is obvious that such layers cannot be produced by bombarding surfaces with energetic atomic carbon and hydrogen, since this mechanism would lead to a ratio in the range of 0.4 at room temperature and the electron temperatures stated above [5]. The same is valid for the layers observed at the lower edges of the Divertor II strike point modules (fig. 4).

References

[1] G. Federici, D. Holland et al., J. Nucl. Mater. **241-243** (1997) 260

[2] H. Maier, S. Kötterl et al., J. Nucl. Mater. **258-263** (1998) 921

[3] D. Naujoks and W. Eckstein, J. Nucl. Mater. **230** (1996) 93

[4] R. Neu, K. Asmussen et al., Plasma Phys. Control. Fusion **38** (1996) A165

[5] W. Jacob, Thin Solid Films **326** (1998) 1